Fluid Phase Equilibria 509 (2020) 112442

Contents lists available at ScienceDirect

Fluid Phase Equilibria

journal homepage: www.elsevier.com/locate/fluid

Viscosity and self-diffusion coefficient of dipolar liquids

S. Nagy [a], D. Balogh [a], I. Szalai [a, b, *]

[a] Institute of Mechatronics Engineering and Research, University of Pannonia, H-8900, Zalaegerszeg, M. Gasparich St. 18/A, Hungary
[b] Institute of Physics and Mechatronics, University of Pannonia, H-8201, Veszprém, PO Box 158, Hungary

ARTICLE INFO

Article history:
Received 30 August 2019
Received in revised form
19 December 2019
Accepted 19 December 2019
Available online 1 January 2020

Keywords:
Dipolar liquids
Viscosity
Self-diffusion
MD simulation
Fluoroalkanes

ABSTRACT

Equilibrium molecular dynamics simulations were used to calculate the viscosity and self-diffusion coefficient of Stockmayer fluids at different dipole moments from the saturated liquid state to the supercritical fluid state. On the basis of the theory of Longuet-Higgins and Pople (J. Chem. Phys. 25 (1956) 884) a physically based correlation equations was proposed for the correlation of density, temperature and dipole moment dependence of viscosity and self-diffusion coefficient simulation data. As an application, with appropriate Stockmayer parameter sets the viscosity of fluoroalkanes were calculated along the saturated liquid curves, and good agreement has been obtained between the experimental and correlation equation data.

1. Introduction

Although computer simulations of viscosity and the self-diffusion coefficient of nonpolar fluids are a well known heading of computational physical chemistry [1–3], only a few papers deal with the corresponding simulation of dipolar model fluids [4–6]. The Lennard-Jones (LJ) potential is one of the simplest model potentials to describe the thermodynamic and transport properties of simple nonpolar fluids. Viscosity and self-diffusion coefficient of this fluid have been studied by molecular dynamics (MD) simulations [7–12]. Because of the importance of this fluid model, the computer simulation data has been correlated by analytical equations. Considering the LJ fluid on the basis of an extension of the Chapman-Enskog theory Rowley and Painter [8] proposed correlation equations for the LJ viscosity and self-diffusion data. Recently, Zabaloy et al. [10–12] slightly modified the parameters and the form of the function of Rowley and Painter [8]. Knowing the LJ parameters, these equations provide moderate description for the pressure and temperature dependence of viscosity and self-diffusion coefficient of different molecular fluids [10,11]. The best known LJ equations of state correlate the free energy of the LJ system (see Refs. [13–16]), but mainly the thermodynamic properties can be calculated from these equations. There exist approaches that relates the equation of state to the transport properties. One of these is the “entropy scaling” devised originally for simple fluids by Rosenfeld [17]. Later this theory was applied for soft spheres [18] for LJ and LJ chainfluids [19–21] and for molecular fluids [22]. The other equation of state based modeling method is the so called “friction theory”, which was proposed by Quinones-Cisneros et al. [23]. On the basis of the corresponding equations of state they calculated the viscosity of *n*-alkanes from methane to *n*-decane. For dipolar fluids the Stockmayer (STM) potential is one of the simplest realistic approximations for the intermolecular interactions. The isotropic (spherically averaged) multipolar potential is a resonable alternative to deal with polar fluids for the calculation of transport and phase equilibrium properties [24]. We mention that Galliero and Boned [25] in their work used a spherically averaged dipolar interaction potential (Keeson potential) instead of the elementary dipole-dipole interaction. According to this choice they could correlate the viscosity data by their Lennard-Jones viscosity correlation equation [26]. To study the density, temperature, and dipole moment dependence of the viscosity and the self-diffusion coefficient of dipolar fluids – similarly to nonpolar fluids – an appropriate theoretically-based correlation equation is necessary.

In this paper, we perform MD simulation for the corresponding transport properties of STM fluids in different thermodynamic liquid states. Starting from the theory of Longuet-Higgins and Pople [27], we complete the LJ correlation equations with a physically-

* Corresponding author. Institute of Mechatronics Engineering and Research, University of Pannonia, H-8900, Zalaegerszeg, M. Gasparich St. 18/A, Hungary.
E-mail address: szalai@almos.vein.hu (I. Szalai).

https://doi.org/10.1016/j.fluid.2019.112442

based new term that correlate the dipolar contributions of the viscosity and the self-diffusion coefficient.

2. Stockmayer potential model for dipolar fluids

At the molecular level the dipolar fluids can be modeled by the STM pair potential which consists of a spherically symmetric LJ potential (characterized by parameters σ and ε)

$$u_{\mathrm{LJ}}(r_{ij}) = 4\varepsilon\left[\left(\frac{\sigma}{r_{ij}}\right)^{12} - \left(\frac{\sigma}{r_{ij}}\right)^{6}\right] \tag{1}$$

and a dipole-dipole (DD) interaction due to point dipoles embedded at the centers of the particles

$$u_{\mathrm{DD}}(\mathbf{r}_{ij}, \omega_i, \omega_j) = -\frac{m^2}{r_{ij}^3} D(\omega_{ij}, \omega_i, \omega_j) \tag{2}$$

with the rotationally invariant function

$$D(\omega_{ij}, \omega_i, \omega_j) = 3(\widehat{\mathbf{m}}_i \widehat{\mathbf{r}}_{ij})(\widehat{\mathbf{m}}_j \widehat{\mathbf{r}}_{ij}) - (\widehat{\mathbf{m}}_i \widehat{\mathbf{m}}_j). \tag{3}$$

In these equations, $r_{ij} = |\mathbf{r}_{ij}|$ is the interparticle distance, $\mathbf{m}_i$ is the dipole moment vector of the ith particle, $m = |\mathbf{m}_i|$ is the strength of the dipole moment, the cap denotes a unit vector, while ω_i and ω_{ij} denote the orientations of vectors $\mathbf{m}_i$ and $\mathbf{r}_{ij}$, respectively.

3. Viscosity and diffusivity of Stockmayer fluids

To correlate our STM shear viscosity simulation data we proceed from the result of Longuet-Higgins and Pople [27] which predicts the following equation for the viscosity of hard sphere fluids:

$$\eta = \frac{2\sigma}{5}\left(\frac{Mk_{\mathrm{B}}T}{\pi}\right)^{1/2} \rho\left(\frac{p}{\rho k_{\mathrm{B}}T} - 1\right), \tag{4}$$

where p is the pressure, ρ is the number density, M is the mass of a particle and k_{B} is the Boltzmann constant. Later, Brown and March [28] suggested the replacement of the pressure, p, with the kinetic pressure $T(\partial p/\partial T)_V$ of the fluid, which is given as

$$T\left(\frac{\partial p}{\partial T}\right)_V = p + \left(\frac{\partial U}{\partial V}\right)_T, \tag{5}$$

where U is the internal energy of the system. This method provides an extension of Eq. (4) to fluids that have attractive interaction potential besides the repulsive hard sphere one. (For hard-core fluids the pressure and the kinetic pressure are the same because $(\partial U/\partial V)_T = 0$.) Using this method Osman et al. [29] have proposed a theory to study the shear viscosity of the hard-core Yukawa fluid. On the basis of the definition of the compressibility factor z it is easy to see, that

$$T\left(\frac{\partial p}{\partial T}\right)_V = \rho k_{\mathrm{B}}T\left(z + T\left(\frac{\partial z}{\partial T}\right)_V\right), \tag{6}$$

where $z = pV/(Nk_{\mathrm{B}}T)$. If we replace p in Eq. (4) with $T(\partial p/\partial T)_V$ of Eq. (6), we obtain that

$$\eta = \frac{2\sigma}{5}\left(\frac{Mk_{\mathrm{B}}T}{\pi}\right)^{1/2} \rho\left(z + T\left(\frac{\partial z}{\partial T}\right)_V - 1\right). \tag{7}$$

We note that for hard spheres $(\partial z/\partial T)_V = 0$, therefore, Eq. (7) reduces to Eq. (4) in this case. For interactions potentials consisting of a hard-core and an excess (repulsive and/or attractive) interaction potentials the compressibility factor can also be divided into two parts:

$$z = z_{\mathrm{hs}}(\rho) + z_{\mathrm{exc}}(\rho, T), \tag{8}$$

therefore, the viscosity of such systems is

$$\eta = \frac{2\sigma}{5}\left(\frac{Mk_{\mathrm{B}}T}{\pi}\right)^{1/2} \rho\left(z_{\mathrm{hs}} + z_{\mathrm{exc}} + T\left(\frac{\partial z_{\mathrm{exc}}}{\partial T}\right)_V - 1\right). \tag{9}$$

According to the perturbation theory of Zwanzig [30], we can formally apply this equation to the calculation of the viscosity of the LJ fluids:

$$\eta_{\mathrm{LJ}} = \frac{2\sigma}{5}\left(\frac{Mk_{\mathrm{B}}T}{\pi}\right)^{1/2} \rho\left(z_{\mathrm{hs}} + z_{\mathrm{exc}}^{\mathrm{LJ}} + T\left(\frac{\partial z_{\mathrm{exc}}^{\mathrm{LJ}}}{\partial T}\right)_V - 1\right), \tag{10}$$

where z_{hs} is the Carnahan-Starling compressibility factor and $z_{\mathrm{exc}}^{\mathrm{LJ}}$ is the excess compressibility factor of the LJ system calculated from a perturbation theory. To express the viscosity of a STM fluid we proceed from one of our earlier results. Within the framework of the perturbation theory and the mean spherical approximation (MSA) we have proposed an equation for the compressibility factor of STM fluids [31,32]:

$$z_{\mathrm{STM}} = z_{\mathrm{hs}} + z_{\mathrm{exc}}^{\mathrm{LJ}} + z_{\mathrm{exc}}^{\mathrm{DD}}. \tag{11}$$

Therefore, for the viscosity of STM fluids we can write that

$$\eta_{\mathrm{STM}} = \frac{2\sigma}{5}\left(\frac{Mk_{\mathrm{B}}T}{\pi}\right)^{1/2} \times \rho\left(z_{\mathrm{hs}} + z_{\mathrm{exc}}^{\mathrm{LJ}} + z_{\mathrm{exc}}^{\mathrm{DD}} - 1 + T\left(\frac{\partial z_{\mathrm{exc}}^{\mathrm{LJ}}}{\partial T}\right)_V + T\left(\frac{\partial z_{\mathrm{exc}}^{\mathrm{DD}}}{\partial T}\right)_V\right). \tag{12}$$

From Eqs. (10) and (12) the viscosity of a STM fluid can be expressed as

$$\eta_{\mathrm{STM}}(\rho, T, m) = \eta_{\mathrm{LJ}}(\rho, T) + \eta_{\mathrm{exc}}^{\mathrm{DD}}(\rho, T, m), \tag{13}$$

where

$$\eta_{\mathrm{exc}}^{\mathrm{DD}}(\rho, T, m) = \frac{2\sigma}{5}\rho\left(\frac{Mk_{\mathrm{B}}T}{\pi}\right)^{1/2}\left(z_{\mathrm{exc}}^{\mathrm{DD}} + T\left(\frac{\partial z_{\mathrm{exc}}^{\mathrm{DD}}}{\partial T}\right)_V\right) \tag{14}$$

is an excess viscosity term, which microscopically depends on the DD interaction. Our aim is to express the explicit ρ, T and m dependence of the $\eta_{\mathrm{exc}}^{\mathrm{DD}}$ term in order to correlate our viscosity simulation data. With this object in Eq. (14) we are going to use the following MSA excess dipolar compressibility factor, which was derived in Ref. [31]:

$$z_{\mathrm{exc}}^{\mathrm{DD}} = \frac{2}{\phi} I(\xi(y)) - \frac{3}{\phi} y\xi(y), \tag{15}$$

where $\phi = \frac{\pi}{6}\sigma^3\rho$ is the packing fraction, y is the dipole strength function

$$y=\frac{4\pi}{9}\frac{\rho\, m^2}{k_BT}, \tag{16}$$

and $I(x)$ is the corresponding MSA function, which comes from the free energy route

$$I(x)=\frac{8}{3}x^2\left[\frac{(1+x)^2}{(1-2x)^4}+\frac{(2-x)^2}{8(1+x)^4}\right]. \tag{17}$$

The parameter $\xi=\xi(y)$ stems from the dipolar hard sphere MSA theory and it is given by the implicit equation

$$3y=\frac{(1+4\xi)^2}{(1-2\xi)^4}-\frac{(1-2\xi)^2}{(1+\xi)^4}. \tag{18}$$

Since z_{exc}^{DD} is an implicit function of y, for an explicit function on the basis of Eq. (18) the following power expansion for $\xi(y)$ is used

$$\xi=\frac{1}{8}y-\frac{15}{256}y^2-\frac{3}{4096}y^3+\dots. \tag{19}$$

The corresponding formula for the $I(y)$ function is

$$I(y)=\frac{1}{16}y^2-\frac{5}{256}y^3-\frac{3}{16384}y^4+\dots \tag{20}$$

Note that the second order power expansion coefficients first were given by Rushbrooke et al. [33]. In Ref. [31] we assessed that in Eq. (15) the packing fraction is temperature dependent through the temperature dependent Barker-Henderson hard sphere diameter ($\sigma=\sigma(T)$). Because we would like to obtain a simple physically based correlation equation for the viscosity, the temperature dependence of the packing fraction is neglected here. Using Eqs. (15), (19) and (20) for the excess compressibility, in the third order, we obtain that

$$z_{exc}^{DD}=-\frac{8}{27}\frac{\pi}{\sigma^3}\frac{\rho m^4}{(k_BT)^2}+\frac{35}{486}\frac{\pi^2}{\sigma^3}\frac{\rho^2m^6}{(k_BT)^3}+\frac{5}{11664}\frac{\pi^3}{\sigma^3}\frac{\rho^3m^8}{(k_BT)^4}. \tag{21}$$

In Eq. (14) the sum of the compressibility factor and its temperature derivative appear. The corresponding result for this expression is

$$z_{exc}^{DD}+T\left(\frac{\partial z_{exc}^{DD}}{\partial T}\right)_V=\frac{8}{27}\frac{\pi}{\sigma^3}\frac{\rho m^4}{(k_BT)^2}-\frac{70}{486}\frac{\pi^2}{\sigma^3}\frac{\rho^2m^6}{(k_BT)^3}-\frac{15}{11664}\frac{\pi^3}{\sigma^3}\frac{\rho^3m^8}{(k_BT)^4}. \tag{22}$$

Substituting Eq. (22) into Eq. (14) the reduced excess viscosity is obtained as

$$\left(\eta_{exc}^{DD}\right)^*=\frac{16\pi^{1/2}}{135}\frac{(\rho^*)^2(m^*)^4}{(T^*)^{3/2}}-\frac{14\pi^{3/2}}{243}\frac{(\rho^*)^3(m^*)^6}{(T^*)^{5/2}}-\frac{\pi^{5/2}}{1944}\frac{(\rho^*)^4(m^*)^8}{(T^*)^{7/2}}, \tag{23}$$

where $\eta_{exc}^*=\eta_{exc}^{DD}\sigma^2/\sqrt{M\varepsilon}$, $\rho^*=\rho\sigma^3$ is the reduced density, $T^*=k_BT/\varepsilon$ is the reduced temperature, and $m^*=m/\sqrt{\varepsilon\sigma^3}$ is the reduced dipole moment. In the following, apart from the constants of this expression, we employ Eq. (23) as a correlation equation, i.e., our excess simulation data are fitted by

$$\left(\eta_{exc}^{DD}\right)^*=a_1\frac{(\rho^*)^2(m^*)^4}{(T^*)^{3/2}}+a_2\frac{(\rho^*)^3(m^*)^6}{(T^*)^{5/2}}+a_3\frac{(\rho^*)^4(m^*)^8}{(T^*)^{7/2}}, \tag{24}$$

where a_1, a_2, a_3 are the fitting parameters. According to this equation the reduced viscosity of a STM fluid can be expressed as

$$\eta_{STM}^*(\rho^*,T^*,m^*)=\eta_{LJ}^*(\rho^*,T^*)+\eta_{exc}^{DD*}(\rho^*,T^*,m^*), \tag{25}$$

where η_{LJ}^* is the reduced viscosity of the LJ fluid. In this work, we employ the correlation equation of Zabaloy et al. ([10]) for the calculation of viscosity of LJ fluid. To correlate the self-diffusion coefficients of the STM liquids, we can follow this route and start from the corresponding equation of Longuet-Higgins and Pople [27]:

$$D=\frac{\sigma}{4}\left(\frac{\pi k_BT}{M}\right)^{1/2}\left(\frac{p}{\rho k_BT}-1\right)^{-1}, \tag{26}$$

where D is the self-diffusion coefficient. After repeating our previous train of thought, we get the following equation for the self-diffusion coefficient of the STM fluid

$$\frac{1}{D_{STM}(\rho,T,m)}=\frac{1}{D_{LJ}(\rho,T)}+\frac{1}{D_{exc}^{DD}(\rho,T,m)}, \tag{27}$$

where D_{exc}^{DD} is due to the DD interaction

$$\frac{1}{D_{exc}^{DD}(\rho,T,m)}=\frac{4}{\sigma}\left(\frac{M}{\pi k_BT}\right)^{1/2}\left(z_{exc}^{DD}+T\left(\frac{\partial z_{exc}^{DD}}{\partial T}\right)_V\right). \tag{28}$$

Using Eq. (22) the DD interaction contribution to the self-diffusion coefficient in reduced units is

$$\frac{1}{\left(D_{exc}^{DD}\right)^*}=\frac{32\pi^{1/2}}{27}\frac{\rho^*(m^*)^4}{(T^*)^{5/2}}-\frac{140\pi^{3/2}}{243}\frac{(\rho^*)^2(m^*)^6}{(T^*)^{7/2}}-\frac{15\pi^{5/2}}{2916}\frac{(\rho^*)^3(m^*)^8}{(T^*)^{9/2}}, \tag{29}$$

where $(D_{exc}^{DD})^*=D_{exc}^{DD}\sqrt{M/(\varepsilon\sigma^2)}$ is the reduced excess self-diffusion coefficient. As in the case of viscosity, we employ Eq. (29) as a correlation equation, i.e. our excess simulation data are fitted by

$$\frac{1}{\left(D_{exc}^{DD}\right)^*}=b_1\frac{\rho^*(m^*)^4}{(T^*)^{5/2}}+b_2\frac{(\rho^*)^2(m^*)^6}{(T^*)^{7/2}}+b_3\frac{(\rho^*)^3(m^*)^8}{(T^*)^{9/2}}, \tag{30}$$

where b_1, b_2 and b_3 are fitting parameters. According to this equation the reduced self-diffusion coefficient of a STM fluid can be expressed as

$$\frac{1}{D_{STM}^*(\rho^*,T^*,m^*)}=\frac{1}{D_{LJ}^*(\rho^*,T^*)}+\frac{1}{D_{exc}^{DD*}(\rho^*,T^*,m^*)}, \tag{31}$$

where D_{LJ}^* is the reduced self-diffusion coefficient of the LJ fluid. For the calculation of self-diffusion coefficient of LJ fluid the correlation equation of Zabaloy et al. [11] is employed.

4. Computer simulation

Equilibrium MD simulations were performed in a cubic box of volume V containing $N_p = 512$ STM particles. The temperature of the system was controlled by using a Berendsen thermostat [34]. For the LJ interaction potential a half-cell cut-off was used. Long-range corrections to the DD interaction were calculated using the reaction field method. The simulations were started from a hcp lattice configuration with randomly oriented dipoles. The equations of motion were integrated using a modified Verlet algorithm [35]. The time step for this algorithm was set to $\Delta t^* = \Delta t\sqrt{\varepsilon/(\sigma^2 M)} = 4 \times 10^{-3}$. (Using the molecular parameters of difluoromethane this reduced time step in real time scale corresponds to $\Delta t \simeq 0.01$ ps.) The simulations were equilibrated over 10^5 time steps, which is in agreement with the equilibration time of Zhang et al. [36], where $t_e \simeq 1$ ns. The production simulations were run with at least 5×10^6 times steps. The statistical uncertainty was estimated using the block average technique using 15–20 blocks. The self-diffusion coefficient, D, of the particles was calculated on the basis of the Green-Kubo relation

$$D = \frac{1}{3N}\int_0^\infty dt\langle \sum_{i=1}^{N}(\mathbf{v}_i(t)\mathbf{v}_i(0))\rangle \tag{32}$$

where t is the time and the brackets $\langle\ldots\rangle$ denote the ensemble average of the velocity autocorrelation function. To eliminate the effect of the periodic boundary condition from the displacement the method given by Rapaport [34] was used. We corrected the diffusion coefficients of a finite periodic system (D_{PBC}) by the hydrodynamic self-interaction term given by Yeh and Hummer [37]:

$$D = D_{PCB} + \frac{k_B T\xi}{6\pi\eta L}, \tag{33}$$

where L is the length of the cubic simulation box and $\xi = 2.837297$. Using our reduced quantities Eq. (33) can be written as:

$$D = D_{PCB} + \frac{(\rho^*)^{1/3}T^*}{6\pi\eta^* N_p^{1/3}}\xi. \tag{34}$$

The shear viscosity was calculated by integrating the time-autocorrelation function of the off-diagonal elements of the stress tensor:

$$\eta = \frac{V}{k_B T}\int_0^\infty dt\langle P_{ab}(t)P_{ab}(0)\rangle, \tag{35}$$

where $a, b \in (x, y, z)$ and P_{ab} is an element of the stress tensor. The statistics of the ensemble average in Eq. (35) were improved by using the independent elements of the stress tensor, i.e. P_{xy}, P_{xz} and P_{yz}. Further statistical improvement in the calculated shear viscosity can be achieved by averaging over six independent terms of the pressure tensor [38,39]). The component P_{ab} is given by

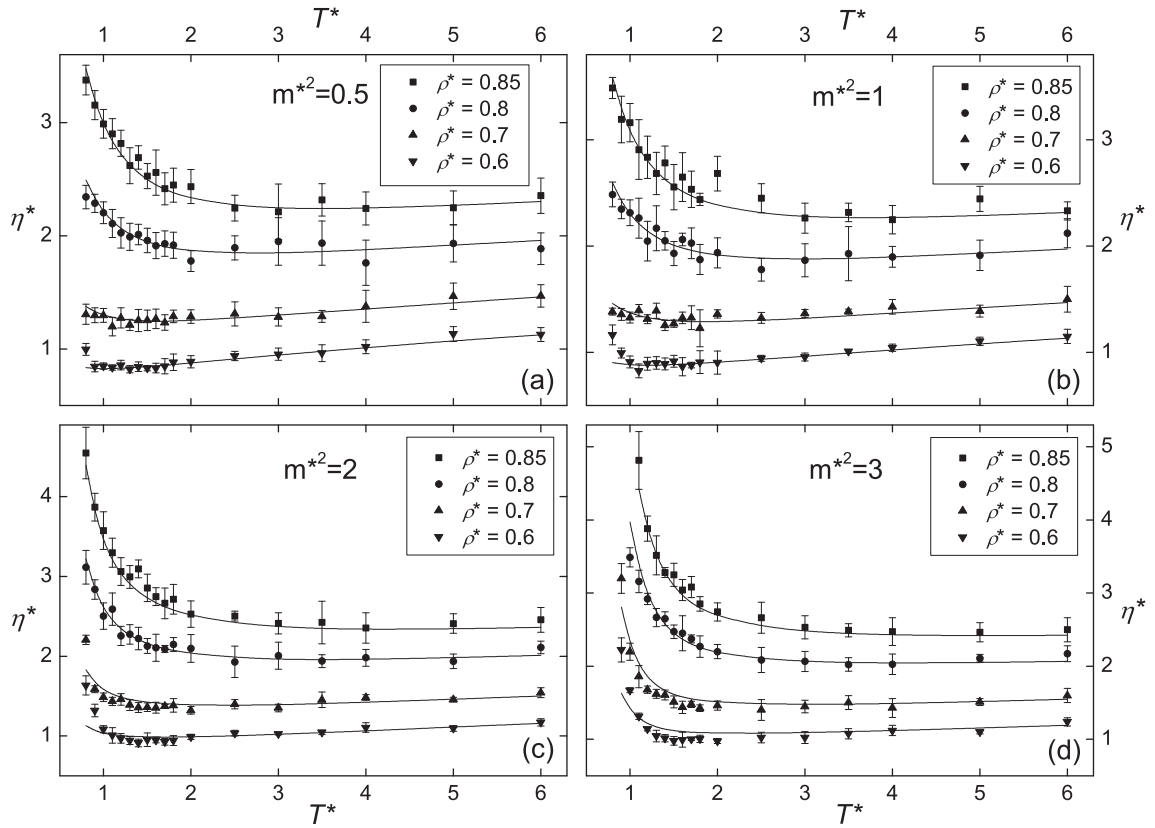

Fig. 1. Viscosity of STM fluids as a function of temperature at varying density values for dipole moments $m^{*2} = 0.5$, $m^{*2} = 1$, $m^{*2} = 2$, and $m^{*2} = 3$. Symbols – with error bars – denotes MD simulation results. Solid lines correspond to Eq. (25).

$$P_{ab} = \frac{1}{V}\left(M\sum_{i=1}^{N} v_{ia}v_{ib} + \frac{1}{2}\sum_{i=1}^{N}\sum_{j\neq i}^{N} r_{ija}f_{ijb}\right), \quad (36)$$

where v_{ia} is the ath component of the velocity of ith particle, while r_{ija} and f_{ija} are the ath component of the inter-particle distance and force vectors between the ith and the jth particles. In the Green-Kubo integral (Eq. (35)) the pressure tensor autocorrelation function decays to zero in the long time limit and the corresponding integral will reach a constant value, which corresponds to the calculated shear viscosity. For our systems we found that after $N \simeq 5 \times 10^3$ time steps the autocorrelation functions practically decay to zero, therefore we cut off the time scale after $N_{cut} \simeq 5\times 10^4$ time steps. (The corresponding real cutoff time is $t_{cut} \simeq 500$ ps, which is smaller than the cutoff time of Zang et al. [36]. We found that in our case the smaller cutoff time is satisfactory, because our molecular model is much simpler than that of Zang et al. [36].) It means that a production simulation was divided into 100 time windows (one time window contains $N = 5 \times 10^4$ time steps) and we calculated the corresponding autocorrelation function trajectory in all windows. After that we calculated the average of 100 autocorrelation function trajectories to decrease the long time noise. The viscosity was calculated from the time integration of the averaged autocorrelation function trajectory. We performed this procedure in all thermodynamic state points.

5. Results and discussion

In this section, the simulation and theoretical predictions for shear viscosity and self-diffusion coefficient of STM fluids are summarized. The majority of the investigated STM fluid state points are in the stable one-phase liquid region. On the (ρ^*, T^*) plane it means that at a given density the corresponding temperature is above the spinodal temperature. We note that while the different LJ equations of state (see Refs. [13–15]) define practically the same spinodal line, the placement of the spinodal lines of STM systems strongly depend on the applied theory [40]. We studied the temperature dependence (at sub- and supercritical temperatures) of both quantities along different liquid isochores with different dipole moments. To our best knowledge, there is no systematic simulation study in the literature for the viscosity of STM fluids, therefore, we summarize the corresponding data in Fig. 1 and Table 1. The excess simulation data are correlated on the basis of Eq. (24), and the corresponding fitting parameters are collected in Table 2. The comparison between the MD simulation and correlation equation data (see Eq. (12)) is shown in Fig. 1. Here the LJ part of the viscosity is described by the correlation equation of [11]. The agreement between the correlation equation and the simulation data is good. At higher densities ($\rho^* = 0.85, 0.8$) close to the liquid-vapor spinodal line the viscosity is increased with decreasing temperatures, while we can see a very weak increase above the corresponding critical temperatures. The dipole moment

Table 1
Molecular dynamics simulation results for viscosity of STM fluids at four different dipole moments and densities in wide range of temperature.

$(m^*)^2$	0.5				1.0				2.0				3.0			
$T^*\backslash\rho^*$	0.6	0.7	0.8	0.85	0.6	0.7	0.8	0.85	0.6	0.7	0.8	0.85	0.6	0.7	0.8	0.85
0.8	0.995 (52)	1.306 (89)	2.342 (104)	3.375 (131)	1.164 (92)	1.383 (33)	2.485 (117)	3.487 (99)	1.634 (120)	2.206 (58)	3.116 (213)	4.548 (321)				
0.9	0.844 (46)	1.297 (65)	2.287 (80)	3.154 (129)	0.993 (46)	1.358 (56)	2.348 (92)	3.191 (219)	1.320 (78)	1.587 (42)	2.837 (123)	3.869 (173)	2.22 4 (165)	3.201 (203)		
1.0	0.848 (28)	1.297 (62)	2.204 (96)	2.989 (127)	0.910 (56)	1.327 (51)	2.313 (121)	3.161 (180)	1.085 (46)	1.486 (55)	2.502 (165)	3.575 (237)	1.671 (34)	2.199 (117)	3.49 (1 30)	
1.1	0.835 (23)	1.197 (83)	2.107 (124)	2.901 (132)	0.826 (66)	1.393 (57)	2.262 (188)	2.907 (280)	1.008 (98)	1.435 (52)	2.591 (202)	3.299 (181)	1.313 (43)	1.857 (150)	3.158 (153)	4.815 (396)
1.2	0.857 (42)	1.274 (89)	2.025 (133)	2.816 (115)	0.893 (61)	1.312 (43)	2.046 (187)	2.834 (199)	0.968 (60)	1.459 (72)	2.255 (122)	3.061 (174)	1.142 (28)	1.678 (49)	2.92 (7 5)	3.881 (172)
1.3	0.821 (32)	1.212 (50)	1.990 (120)	2.620 (159)	0.900 (59)	1.391 (72)	2.168 (211)	2.683 (198)	0.943 (48)	1.388 (69)	2.275 (122)	2.994 (142)	1.04 5 (79)	1.621 (60)	2.666 (125)	3.516 (268)
1.4	0.842 (42)	1.252 (98)	2.010 (91)	2.691 (103)	0.891 (57)	1.253 (47)	2.048 (87)	2.782 (157)	0.912 (48)	1.356 (61)	2.222 (141)	3.096 (113)	1.015 (50)	1.607 (68)	2.649 (93)	3.282 (68)
1.5	0.830 (23)	1.252 (90)	1.957 (108)	2.526 (111)	0.916 (55)	1.270 (35)	1.93 (113)	2.554 (212)	0.953 (84)	1.361 (52)	2.127 (93)	2.857 (170)	0.980 (58)	1.513 (82)	2.472 (93)	3.250 (158)
1.6	0.831 (42)	1.265 (86)	1.912 (115)	2.558 (200)	0.865 (86)	1.324 (53)	2.062 (60)	2.647 (230)	0.949 (34)	1.354 (67)	2.106 (168)	2.748 (112)	0.994 (101)	1.437 (84)	2.451 (238)	3.042 (146)
1.7	0.847 (66)	1.233 (69)	1.930 (112)	2.415 (141)	0.880 (26)	1.326 (113)	2.026 (144)	2.533 (170)	0.927 (41)	1.375 (19)	2.091 (42)	2.663 (194)	1.001 (16)	1.479 (43)	2.375 (55)	3.082 (145)
1.8	0.882 (72)	1.287 (56)	1.916 (115)	2.447 (150)	0.908 (108)	1.227 (173)	1.873 (141)	2.438 (58)	0.942 (63)	1.383 (84)	2.148 (88)	2.714 (187)	1.007 (50)	1.425 (46)	2.268 (148)	2.853 (101)
2.0	0.886 (53)	1.286 (61)	1.776 (92)	2.434 (150)	0.904 (108)	1.361 (38)	1.937 (141)	2.681 (162)	0.989 (33)	1.321 (48)	2.098 (174)	2.527 (165)	0.975 (33)	1.463 (63)	2.200 (98)	2.743 (125)
2.5	0.937 (40)	1.310 (107)	1.893 (107)	2.243 (114)	0.944 (28)	1.324 (51)	1.778 (107)	2.449 (137)	1.035 (35)	1.399 (57)	1.930 (197)	2.502 (62)	1.023 (72)	1.402 (143)	2.084 (171)	2.663 (212)
3.0	0.953 (53)	1.283 (81)	1.949 (211)	2.212 (244)	0.957 (37)	1.367 (37)	1.867 (155)	2.262 (141)	1.026 (13)	1.351 (47)	2.006 (169)	2.412 (133)	1.024 (82)	1.448 (85)	2.066 (138)	2.533 (158)
3.5	0.963 (74)	1.287 (53)	1.934 (196)	2.317 (143)	1.010 (18)	1.384 (24)	1.928 (254)	2.317 (87)	1.045 (26)	1.453 (98)	1.939 (82)	2.424 (267)	1.076 (70)	1.503 (96)	2.023 (93)	2.491 (91)
4.0	1.020 (62)	1.376 (142)	1.761 (200)	2.241 (146)	1.043 (34)	1.429 (68)	1.898 (97)	2.247 (133)	1.106 (60)	1.482 (35)	1.980 (104)	2.354 (189)	1.119 (70)	1.428 (129)	2.026 (140)	2.474 (190)
5.0	1.132 (66)	1.465 (117)	1.931 (163)	2.247 (148)	1.104 (38)	1.388 (57)	1.912 (143)	2.442 (118)	1.094 (36)	1.456 (30)	1.938 (91)	2.409 (122)	1.100 (26)	1.510 (46)	2.109 (52)	2.464 (130)
6.0	1.128 (61)	1.468 (100)	1.885 (140)	2.354 (156)	1.150 (67)	1.500 (122)	2.120 (137)	2.331 (85)	1.171 (45)	1.544 (62)	2.111 (78)	2.456 (154)	1.239 (55)	1.599 (97)	2.170 (109)	2.499 (166)

Table 2
The fitted coefficients a_i and b_i in Eq. (24) and Eq. (30).

	$i=1$	$i=2$	$i=3$
a_i	0.4214	−0.3811	0.1401
b_i	2.5306	−1.8578	0.4584

dependence of the critical temperature of STM fluids was given by Bartke end Hentschke [41], who obtained the following data via MD simulations: ($m^{*2}=0.5$, $T_c^*=1.39$), ($m^{*2}=1$, $T_c^*=1.45$), ($m^{*2}=2$, $T_c^*=1.65$) and ($m^{*2}=3$, $T_c^*=1.86$). Fig. 1 shows that in the same state points the viscosity increases with increasing dipole moment (it can be seen most significantly via the comparison of Fig. 1(a) and (d)). We note that in the case of Fig. 1(c) and (d) at low temperatures ($T^*\approx 1$) the corresponding state points (ρ^*, T^*) probably are in the two-phase region (they are below the spinodal line), therefore, there is only a moderate agreement between the MD simulation data and the correlation equation data.

In Table 3 and Fig. 2 we show the self-diffusion coefficient simulation data for the STM fluids with different reduced dipole moments. Fig. 2 shows the temperature and density dependence of the simulation data in comparison with the corresponding correlation equation data (see Eqs. (31) and (30)). The fitted parameters of the self-diffusion correlation equation are collected in Table 2. We can see that in the studied liquid phase at a given density and dipole moment the self-diffusion coefficient is a monotonically increasing function of the temperature. At a given temperature the self-diffusion coefficient decreases with increasing densities. Fig. 2 and Table 3 show that in the same state points the self-diffusion coefficient decreases with increasing dipole moment (it can be seen most significantly via the comparison of Fig. 2(a) and (d)).

As an application, we show a few results for our viscosity correlation equation in comparison with experimental data. Fig. 3 shows the experimental viscosity data for saturated fluoroalkanes and the corresponding correlation equation results. The experimental data references are shown in Table 4. The STM potential parameters ($\sigma_G, \varepsilon_G, m_G^*$) have been taken from Gao et al. [46]. They obtained these data from Gibbs ensemble simulations of vapor-liquid equilibria of fluoroalkanes. Using these parameter sets, our correlation equation reproduces the experimental data only at high temperatures. This is not too surprising because the thermodynamic parameter sets are applied to calculate the transport properties of the system. To have better agreement we retained the LJ part (Gao et al. [46]) of the STM parameters and refitted only dipole moments. The corresponding new dipole moments (m_N^*) are also summarized in Table 4. As Fig. 3(a–d) show, using these new parameter sets we could describe the temperature dependence of viscosity of different materials along the saturated liquid curves with reasonable agreement. Regarding R134a fluid the agreement

Table 3
Molecular dynamics simulation results for self-diffusion coefficient of STM fluids at for different dipole moments and densities in wide range of temperature.

$(m^*)^2$	0.5				1.0				2.0				3.0			
$T^*\backslash\rho^*$	0.6	0.7	0.8	0.85	0.6	0.7	0.8	0.85	0.6	0.7	0.8	0.85	0.6	0.7	0.8	0.85
0.8	0.1044 (25)	0.0904 (19)	0.0536 (19)	0.0384 (8)	0.0854 (28)	0.08376 (18)	0.0510 (15)	0.0359 (11)	0.0563 (33)	0.0549 (22)	0.0452 (11)	0.0337 (12)				
0.9	0.1485 (33)	0.1038 (28)	0.0618 (21)	0.0453 (11)	0.1221 (22)	0.0977 (26)	0.0590 (14)	0.0434 (11)	0.0803 (34)	0.0841 (32)	0.0535 (15)	0.0407 (13)	0.0571 (36)	0.0556 (20)		
1.0	0.1724 (40)	0.1172 (26)	0.0714 (24)	0.0535 (12)	0.1615 (35)	0.1128 (34)	0.0685 (21)	0.0510 (13)	0.1142 (43)	0.1004 (12)	0.0628 (10)	0.0469 (11)	0.0782 (29)	0.0784 (30)	0.0583 (20)	
1.1	0.1910 (47)	0.1301 (32)	0.0808 (13)	0.0614 (21)	0.1794 (49)	0.1205 (18)	0.0762 (19)	0.589 (20)	0.1518 (35)	0.1112 (22)	0.0709 (21)	0.0544 (12)	0.1058 (40)	0.1009 (24)	0.0666 (18)	0.0509 (15)
1.2	0.2072 (52)	0.1414 (35)	0.0896 (26)	0.0685 (17)	0.1973 (37)	0.1355 (23)	0.0867 (18)	0.0658 (22)	0.1744 (45)	0.1239 (30)	0.0797 (24)	0.0620 (12)	0.1403 (41)	0.1131 (31)	0.0737 (17)	0.0588 (19)
1.3	0.2248 (49)	0.1529 (25)	0.0984 (27)	0.0768 (17)	0.2130 (38)	0.1454 (41)	0.0939 (26)	0.0744 (21)	0.1921 (40)	0.1354 (43)	0.0863 (21)	0.0684 (19)	0.1725 (48)	0.1253 (23)	0.0829 (16)	0.0650 (23)
1.4	0.2429 (52)	0.1668 (35)	0.1073 (20)	0.0833 (17)	0.2274 (46)	0.1608 (29)	0.1038 (18)	0.0812 (21)	0.2059 (31)	0.1465 (37)	0.0960 (18)	0.0761 (25)	0.1874 (29)	0.1346 (33)	0.0897 (36)	0.0716 (22)
1.5	0.2576 (46)	0.1774 (30)	0.1187 (26)	0.0917 (26)	0.2420 (49)	0.1702 (50)	0.1138 (22)	0.0882 (13)	0.2274 (54)	0.1601 (23)	0.1058 (21)	0.0837 (18)	0.2042 (42)	0.1457 (36)	0.0988 (29)	0.0770 (20)
1.6	0.2730 (50)	0.1886 (37)	0.1256 (21)	0.0988 (22)	0.2595 (45)	0.1806 (45)	0.1206 (28)	0.0958 (16)	0.2373 (85)	0.1674 (40)	0.1128 (12)	0.0912 (17)	0.2202 (72)	0.1552 (32)	0.1057 (31)	0.0858 (10)
1.7	0.2826 (85)	0.1998 (46)	0.1344 (31)	0.1073 (16)	0.2763 (37)	0.1918 (37)	0.1306 (24)	0.1039 (15)	0.2549 (58)	0.1798 (19)	0.1226 (22)	0.0962 (26)	0.2362 (54)	0.1669 (26)	0.1134 (15)	0.0919 (27)
1.8	0.3003 (70)	0.2138 (65)	0.1438 (24)	0.1170 (27)	0.2887 (39)	0.2060 (47)	0.1404 (40)	0.1120 (24)	0.2664 (56)	0.1913 (50)	0.1294 (48)	0.1061 (30)	0.2478 (53)	0.1780 (28)	0.1224 (26)	0.1009 (19)
2.0	0.3255 (44)	0.2334 (41)	0.1627 (41)	0.1322 (23)	0.3187 (106)	0.2242 (58)	0.1571 (42)	0.1264 (24)	0.2952 (58)	0.2160 (58)	0.1474 (18)	0.1196 (10)	0.2768 (63)	0.1996 (42)	0.1394 (19)	0.1129 (24)
2.5	0.3893 (83)	0.2885 (51)	0.2054 (72)	0.1697 (38)	0.3868 (64)	0.2804 (54)	0.1985 (30)	0.1641 (29)	0.3593 (85)	0.2650 (75)	0.1909 (33)	0.1564 (36)	0.3428 (69)	0.2543 (67)	0.1785 (34)	0.1486 (50)
3.0	0.4556 (92)	0.3356 (51)	0.2444 (66)	0.2086 (48)	0.4467 (61)	0.3334 (78)	0.2425 (41)	0.2013 (38)	0.4264 (114)	0.3188 (64)	0.2291 (70)	0.1944 (37)	0.4052 (79)	0.3023 (71)	0.2203 (47)	0.1872 (48)
3.5	0.5154 (84)	0.3901 (97)	0.2861 (64)	0.2402 (50)	0.5067 (99)	0.3816 (50)	0.2814 (67)	0.2375 (36)	0.4922 (100)	0.3644 (84)	0.2673 (93)	0.2260 (48)	0.4681 (112)	0.3466 (61)	0.2571 (23)	0.2218 (24)
4.0	0.5784 (165)	0.4335 (78)	0.3309 (69)	0.2788 (44)	0.5698 (119)	0.4291 (66)	0.3200 (47)	0.2730 (62)	0.5473 (98)	0.4103 (86)	0.3088 (56)	0.2617 (48)	0.5250 (103)	0.3971 (54)	0.2961 (90)	0.2550 (60)
5.0	0.6766 (128)	0.5243 (104)	0.3982 (34)	0.3483 (114)	0.6824 (141)	0.5156 (101)	0.3971 (77)	0.3406 (34)	0.6605 (160)	0.5037 (110)	0.3873 (64)	0.3287 (57)	0.6424 (121)	0.4884 (119)	0.3662 (93)	0.3154 (49)
6.0	0.7857 (141)	0.6056 (117)	0.4743 (60)	0.4095 (60)	0.7772 (193)	0.6130 (70)	0.4616 (105)	0.4087 (100)	0.7709 (137)	0.5969 (75)	0.4533 (103)	0.3934 (103)	0.7504 (113)	0.5765 (98)	0.4431 (67)	0.3804 (68)

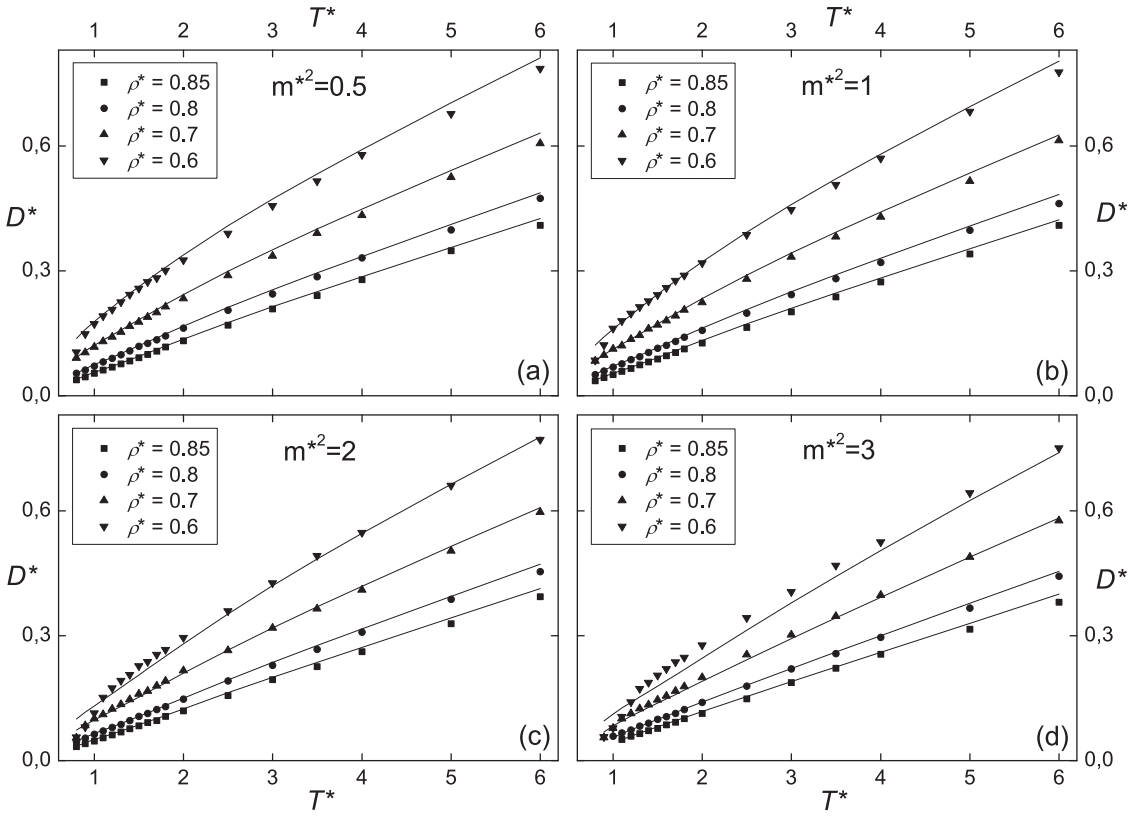

Fig. 2. Self-diffusion coefficient of STM fluids as a function of temperature at varying density values for dipole moments $m^{*2} = 0.5$, $m^{*2} = 1$, $m^{*2} = 2$, and $m^{*2} = 3$. Symbols denotes MD simulation results. The error bars are smaller than the corresponding symbols. Solid lines correspond to Eq. (31).

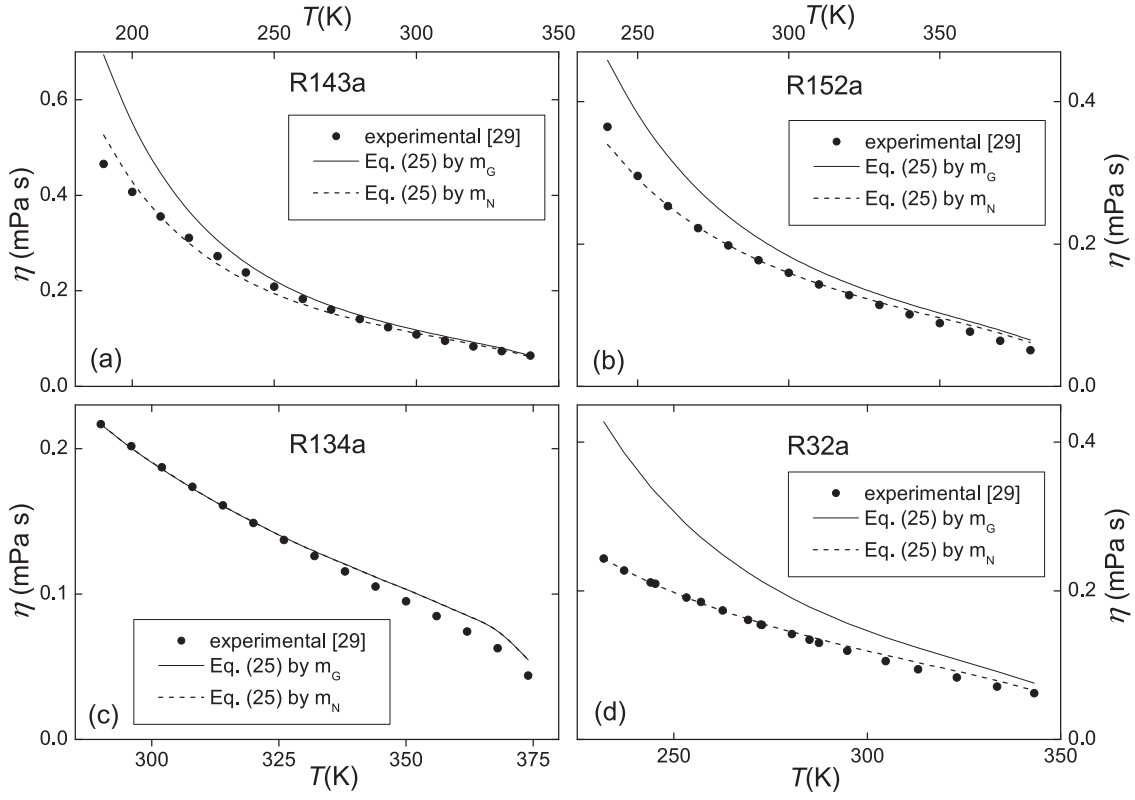

Fig. 3. Viscosity for fluoroalkanes along the saturation curves. Symbols denotes experimental data. The lines correspond to model predictions. Dashed lines describe the viscosity obtained from STM parameters $(\sigma_G, \varepsilon_G, m_G^*)$ of Gao et al. [46]. Solid line describe the viscosity by the same parameters $(\sigma_G, \varepsilon_G)$ and by the refitted dipole moments (m_N^*). The corresponding parameters are summarized in Table 4.

Table 4
The values of STM potential parameters (σ_G, ε_G, m_G^*) from Ref. [46] and the refitted dipole moments (m_N^*) for four fluoroalkane fluids.

Compound	Exp. data	σ_G/Å	(ε_G/k_B)/K	m_G^*	m_N^*
1,1,1-Trifluoroethane (R-143a)	[42]	4.559	169.2	1.990	1.889
1,1-Difluoroethane (R-152a)	[43]	4.458	186.1	2.022	1.884
1,1,1,2-Tetrafluoroethane (R134a)	[44]	4.632	174.9	2.084	2.084
Difluoromethane (R32)	[45]	3.900	163.1	2.098	1.720

between the theoretical viscosity curves is especially satisfactory, because the fitted reduced dipole moment (m_N^*) is equal to the value (m_G^*) given by Ref. [46].

6. Summary

The viscosity and self-diffusion coefficient of STM fluids were described by only 3 plus 3 additional parameters, compared to the corresponding LJ values. The calculation was performed at high density for wide range of temperature and dipole moment. Our correlation equation contains the appropriate powers of density, temperature and dipole moment. Our theory seems to be appropriate for the estimation of the magnitude of the dipole moment of dipolar fluids from experimental viscosity data. Besides the theoretical work hundreds of equilibrium MD simulations were performed to map the transport coefficients for STM fluids whose results are shared.

Declaration of competing interest

The authors declare that they have no known competing _nancial interests or personal relationships that could have appeared to inuence the work reported in this paper.

CRediT authorship contribution statement

S. Nagy: Software, Visualization. **D. Balogh:** Visualization, Validation. **I. Szalai:** Conceptualization, Supervision, Writing - original draft.

Acknowledgements

The project has been supported by the European Union, co-financed by the European Social Fund. EFOP-3.6.2-16-2017-00002. This publication has been supported by the Hungarian Government, Hungary through the Thematic Excellence Program NKFIH-843-10/2019.

References

[1] D.M. Heves, A.C. Branka, Self-diffusion coefficients and shear viscosity of inverse power fluids: from hard-to soft-spheres, Phys. Chem. Chem. Phys. 10 (2008) 4036–4044.
[2] S.T. Cui, P.T. Cummings, H.D. Cochram, The calculation of viscosity of liquid n -decane and n-hexadecane by Green-Kubo method, Mol. Phys. 93 (1998) 117–121.
[3] M.P. Allen, D.J. Tildesley, Computer Simulation of Liquids, Clarendon Press, Oxford, 2001.
[4] A.L. Kielpinsky, K. Mansour, S. Murad, Equilibrium and nonequilibrium computer simulation studies of polar fluids and nonpolar mixtures, Int. J. Thermophys. 7 (1986) 421–430.
[5] G.A. Fernández, J. Vrabec, H. Hasse, Shear viscosity and thermal conductivity of dipolar real fluids from equilibrium molecular dynamics simulation, Cryogenics 46 (2006) 711–717.
[6] J. Bartke, Computer Simulation of the Stockmayer Fluid. PhD Dissertation, Bergische Univerität, Wuppertal, 2008, pp. 193–196.
[7] K. Tankeshwar, K.N. Pathak, S. Ranganathan, The shear viscosity of Lennard-Jones fluids, J. Phys. C Solid State Phys. 21 (1988) 3607–3617.
[8] R.L. Rowley, M.M. Painter, Diffusion and viscosity equations of state for a Lennard-Jones fluid obtained from molecular dynamics simulations, Int. J. Thermophys. 18 (1997) 1109–1121.
[9] G. Galliero, C. Boned, A. Baylaucq, Molecular dynamics study of the Lennard-Jones fluid viscosity: application to real fluids, Ind. Eng. Chem. Res. 44 (2005) 6963–6972.
[10] M.S. Zabaloy, V.R. Vasquez, E.A. Macedo, Viscosity of pure supercritical fluids, J. Supercrit. Fluids 36 (2005) 106–117.
[11] M.S. Zabaloy, V.R. Vasquez, E.A. Macedo, Description of self-diffusion coefficients of gases, liquids and fluids at high pressure based on molecular simulation data, Fluid Phase Equilib. 242 (2006) 43–56.
[12] M.S. Zabaloy, J.M.V. Machado, E.A. Macedo, A study of Lennard-Jones Equivalent Analytical Relationships for modeling viscosities, Int. J. Thermopysics 22 (2001) 829–858.
[13] J.K. Johnson, J.A. Zollweg, K.E. Gubbins, The Lennard-Jones equation of state revisited, Mol. Phys. 78 (1993) 591–618.
[14] M. Mecke, A. Muller, J. Winkelmann, J. Vrabec, J. Fischer, R. Span, W. Wagner, An accurate van der Waals type equation of state for the Lennard-Jones fluid, Int. J. Thermophys. 17 (1996) 391–404.
[15] J. Kolafa, I. Nezbeda, The Lennard-Jones fluid: an accurate analytic and theoretically-based equation of state, Fluid Phase Equilib. 100 (1994) 1–34.
[16] L. Chunxi, L. Yigui, L. Jiufang, Investigation and improvement of equations of state for Lennard-Jones fluid, Fluid Phase Equilib. 127 (1997) 71–81.
[17] Y. Rosenfeld, A quasi-universal scaling law for atomic transport in simple fluids, J. Phys. Condens. Matter 11 (1999) 5415–5427.
[18] S. Pieprzyk, D.M. Heyes, A.C. Branka, Thermodynamic properties and entropy scaling law for diffusivity in soft spheres, Phys. Rev. E 90 (2014), 012106.
[19] O. Lötgering-Lin, M. Fischer, M. Hopp, J. Gross, Pure substance and mixture viscosities based on entropy scaling and an analytic equation of state, Ind. Eng. Chem. Res. 57 (2018) 4095–4114.
[20] I.H. Bell, R. Messerly, M. Thol, L. Costigliola, J.C. Dyre, Modified entropy scaling of the transport properties of the Lennard-Jones fluid, J. Phys. Chem. B 123 (2019) 6345–6363.
[21] G. Galliero, C. Boned, J. Fernández, Scaling of the viscosity of the Lennard-Jones chain fluid model, argon, and some normal alkanes, J. Chem. Phys. 134 (2011), 064505.
[22] W.A. Fouad, L.F. Vega, Transport properties of HFC and HFO based refrigerants using an excess entropy scaling approach, J. Supercrit. Fluids 131 (2018) 106–116.
[23] S.E. Quinones-Cisnores, C.K. Zéberg-Mikkelsen, E.H. Stenby, The friction theory (f-theory) for viscosity modeling, Fluid Phase Equilib. 169 (2000) 249–276.
[24] E.A. Müller, L.D. Gelb, Molecular modeling of fluid-phase equilibria using an isotropic multipolar potential, Ind. Eng. Chem. Res. 42 (2003) 4123–4131.
[25] G. Galliero, C. Boned, Dynamic viscosity estimation of hydrogen sulfide using predictive scheme based on molecular dynamics, Fluid Phase Equilib. 269 (2008) 19–24.
[26] G. Galliero, C. Boned, A. Baylaucq, Molecular dynamics study of Lennard-Jones fluid viscosity: application to real fluids, Ind. Eng. Chem. Res. 44 (2005) 6963–6972.
[27] H.C. Longuet-Higgins, J.A. Pople, Transport properties of dense fluid of hard spheres, J. Chem. Phys. 25 (1956) 884–889.
[28] R.C. Brown, N.H. March, Structure and excitations in liquid and solid surfaces, Phys. Rep. 24 (1976) 77–169.
[29] S.M. Osman, I. Ali, R.N. Singh, Shear viscosity along the liquid-vapour coexistence, J. Phys. Condens. Matter 14 (2002) 8415–8423.
[30] R.W. Zwanzig, High-temperature equation of state by a perturbation method: I. Nonpolar gases, J. Chem. Phys. 22 (1954) 1420–1426.
[31] G. Kronome, J. Liszi, I. Szalai, Mean spherical approximation based perturbation theory equation of state for Stockmayer fluids, J. Chem. Soc., Faraday Trans. 93 (1997) 3053–3059.
[32] I. Szalai, G. Kronome, T. Lukacs, New equation of state for Stockmayer gases, J. Chem. Soc., Faraday Trans. 93 (1997) 3737–3739.
[33] G.S. Rushbrooke, G. Stell, J.S. Høye, Theory of polar liquids. I. Dipolar hard spheres, Mol. Phys. 26 (1973) 1199–1215.
[34] D.C. Rapaport, The Art of Molecular Dynamics Simulation, Cambridge University Press, Cambridge, 1995.
[35] D.M. Heyes, Transport coefficients of Lennard-Jones fluids: a molecular-dynamics and effective-hard-sphere treatment, Phys. Rev. B 37 (1988) 5677.
[36] Y. Zhang, A. Otani, E.J. Maginn, Realible viscosity calculation from equilibrium molecular dynamics simulations: a time decomposition method, J. Chem. Theory Comput. 11 (2015) 3537–3546.
[37] I.-C. Yeh, G. Hummer, System-size dependence of diffusion coefficients and viscosities from molecular dynamics simulations with periodic boundary conditions, J. Phys. Chem. B 108 (2004) 15873–15879.

[38] B.L. Holian, D.J. Evans, Shear viscosities away from the melting line: a comparison of equilibrium and nonequilibrium molecular dynamics, J. Chem. Phys. 78 (1983) 5147–5150.
[39] C. Rey-Castro, L.F. Vegsa, Transport properties of the ionic liquid 1-ethyl-3-Methyllimidazolium chloride from equilibrium molecular dynamics simulation. The effect of temperature, J. Phys. Chem. B 110 (2006) 14426–14435.
[40] S. Klapp, F. Forstmann, Phase transitions in dipolar fluids: an integral equation study, J. Chem. Phys. 106 (1997) 9742–9761.
[41] J. Bartke, R. Hentschke, Phase behavior of the Stockmayer fluid via molecular dynamics simulation, Phys. Rev. E 75 (2007), 061503 1-06150311.
[42] K. Srinivasan, L.R. Oellrich, Saturation properties of the refrigerant 143A, Int. J. Refrig. 20 (1997) 332–338.
[43] R. Krauss, V.C. Weiss, T.A. Edison, J.V. Sengers, K. Stephan, Transport properties of 1.1-Difluoroethane (R152a), Int. J. Thermophys. 17 (1996) 731–757.
[44] R. Krauss, J. Luettmer-Strathmann, J.V. Sengers, K. Stephan, Transport properties of 1,1,1,2-Tetrafluoroethane (R134a), Int. J. Thermophys. 14 (1993) 951–988.
[45] C.M.B.P. Oliveira, W.A. Wakeham, The viscosity of R32 and R125 at saturation, Int. J. Thermophys. 14 (1993) 1131–1143.
[46] G.T. Gao, W. Wang, X.C. Zeng, Gibbs ensemble simulation of HCFC/HFC mixtures by effective Stockmayer potential, Fluid Phase Equilib. 158–160 (1999) 69–78.